Cerebral Cortex March 2009;19:497-510
doi:10.1093/cercor/bhn113
Advance Access publication July 16, 2008

FEATURE ARTICLE

The Cortical Signature of Alzheimer's Disease: Regionally Specific Cortical Thinning Relates to Symptom Severity in Very Mild to Mild AD Dementia and is Detectable in Asymptomatic Amyloid-Positive Individuals

Bradford C. Dickerson[1,2,3,4], Akram Bakkour[5], David H. Salat[3,6], Eric Feczko[5], Jenni Pacheco[3,6], Douglas N. Greve[3,6], Fran Grodstein[7], Christopher I. Wright[3,4,5], Deborah Blacker[2,5], H. Diana Rosas[1,2,3], Reisa A. Sperling[1,2,3,4], Alireza Atri[1,2], John H. Growdon[1,2], Bradley T. Hyman[1,2], John C. Morris[8], Bruce Fischl[3,6,9] and Randy L. Buckner[3,6,10]

[1]Department of Neurology [2]Massachusetts Alzheimer's Disease Research Center [3]Athinoula A. Martinos Center for Biomedical Imaging, Massachusetts General Hospital and Harvard Medical School, Boston, MA, USA [4]Division of Cognitive and Behavioral Neurology, Department of Neurology, Brigham & Women's Hospital, Boston, MA, USA [5]Department of Psychiatry [6]Department of Radiology, Massachusetts General Hospital and Harvard Medical School, Boston, MA, USA [7]Department of Internal Medicine, Brigham & Women's Hospital, Boston, MA, USA [8]Department of Neurology and Alzheimer's Disease Research Center, Washington University School of Medicine, St Louis, MO, USA [9]Computer Science and Artificial Intelligence Laboratory, Massachusetts Institute of Technology, Cambridge, MA, USA and [10]Department of Psychology and Howard Hughes Medical Institute, Harvard University, Cambridge, MA, USA

Alzheimer's disease (AD) is associated with neurodegeneration in vulnerable limbic and heteromodal regions of the cerebral cortex, detectable in vivo using magnetic resonance imaging. It is not clear whether abnormalities of cortical anatomy in AD can be reliably measured across different subject samples, how closely they track symptoms, and whether they are detectable prior to symptoms. An exploratory map of cortical thinning in mild AD was used to define regions of interest that were applied in a hypothesis-driven fashion to other subject samples. Results demonstrate a reliably quantifiable in vivo signature of abnormal cortical anatomy in AD, which parallels known regional vulnerability to AD neuropathology. Thinning in vulnerable cortical regions relates to symptom severity even in the earliest stages of clinical symptoms. Furthermore, subtle thinning is present in asymptomatic older controls with brain amyloid binding as detected with amyloid imaging. The reliability and clinical validity of AD-related cortical thinning suggests potential utility as an imaging biomarker. This "disease signature" approach to cortical morphometry, in which disease effects are mapped across the cortical mantle and then used to define ROIs for hypothesis-driven analyses, may provide a powerful methodological framework for studies of neuropsychiatric diseases.

Keywords: Alzheimer's disease, cerebral cortex, magnetic resonance imaging, medial temporal lobe, parietal cortex

Introduction

The symptoms of Alzheimer's disease (AD)—progressive impairment in memory, executive function, visuospatial abilities, language, and behavior—arise from neurodegeneration of specific brain regions, prominently including the paralimbic and heteromodal association areas. Initially, knowledge of brain regions selectively vulnerable to AD was obtained from post-mortem brain tissue (Brun and Gustafson 1976; Arnold et al. 1991; Braak and Braak 1991; Morrison and Hof 2002). In the past 15 years, magnetic resonance imaging (MRI) has provided insights into quantitative neuroanatomic abnormalities in living individuals with AD as well as the progressive course of the disease. Volume loss in specific regions, such as the hippocampal formation (Jack et al. 1992; Killiany et al. 1993) and entorhinal cortex (Juottonen et al. 1998; Bobinski et al. 1999; Killiany et al. 2000; Dickerson et al. 2001), can be detected in vivo using manual region-of-interest MRI techniques.

Manual methods are labor-intensive and typically focus on a few a priori–defined regions, which has resulted in the extensive study of some regions of the brain that are well known to be affected by AD (e.g., the hippocampal formation and entorhinal cortex) without equivalent study of the distributed network of all brain regions affected. Analysis of differences in whole-brain volume between individuals with early AD and controls (Fotenos et al. 2005) as well as accelerated whole-brain atrophy rates in AD (Fox et al. 1999; Cardenas et al. 2003; Fotenos et al. 2005) make clear that extensive regional changes are taking place in AD because changes localized to the medial temporal lobe simply cannot account for such large-scale effects, which are present even at the earliest stages of the disease. As an extreme example, clinically nondemented individuals (Clinical Dementia Rating [CDR] = 0) with positive amyloid binding as measured using positron emission tomography (PET) show reduced whole-brain volumes relative to amyloid-free peers suggesting that cortical atrophy may be present before clinical symptoms appear (Fotenos et al. 2008).

These observations raise several questions that can be investigated using MRI measures. First, of the spatially distributed cortical regions that are most prominently affected in AD, does the relative magnitude of atrophy suggest a sequence of involvement similar to that hypothesized from post-mortem studies? Is the pattern of vulnerable cortical regions consistent from one group of individuals with AD to the next? And how early in the progression of the disease can differences in vulnerable cortex be detected? The answers to these questions will provide in vivo data about the brain networks affected in AD that can complement neuropathological data as well as identify affected cortical regions for use as biomarkers for detection and monitoring of AD.

© 2008 The Authors
This is an Open Access article distributed under the terms of the Creative Commons Attribution Non-Commercial License (http://creativecommons.org/licenses/by-nc/2.0/uk/) which permits unrestricted non-commercial use, distribution, and reproduction in any medium, provided the original work is properly cited.

Insights into the distributed cortical regions that show atrophy in AD have begun to emerge. Computational MRI data analysis methods based on voxel-based morphometry or analysis of local cortical deformations provide maps of estimated gray matter atrophy in AD without a priori focus on specific regions (Baron et al. 2001; Thompson et al. 2001; Frisoni et al. 2002; Good et al. 2002; Scahill et al. 2002; Karas et al. 2003; Buckner et al. 2005). Consistent with expectations, these studies reveal effects of AD on distributed regions of cortex including posterior lateral temporoparietal and medial parietal regions as well as robust effects in medial and lateral temporal cortex. Methods have also been developed that enable the measurement of cortical thickness across the entire cortical mantle (Fischl and Dale 2000; MacDonald et al. 2000; Kabani et al. 2001; Rosas et al. 2002). Initial studies of cortical thickness demonstrate thinning in distributed association areas again suggesting that regional atrophy can be detected across widespread cortical regions (Lerch et al. 2005; Du et al. 2007). One advantage of the measurement of cortical thickness is that it provides a quantitative value that represents a physical property of the brain that can be measured in an individual person, whether in vivo or from post-mortem tissue (Rosas et al. 2002).

Here we expanded upon prior work on cortical thinning in AD in several important ways. First, although voxel-based studies have included patients with milder forms of AD (Karas

Figure 1. Flowchart of methodologic procedures employed in this study and specific analyses used to generate figures (Fig) and tables (Tbl). Shaded rows at bottom show the specific subject samples (S) that were used to generate each table and figure. For example, Samples 1a and 1b were used to generate Figure 4 and Table 4 (second shaded row). See Table 1 for details of diagnostic groups and demographic and clinical characteristics of each sample.

Table 1
Demographic and clinical characteristics of participants

Sample		Group	*N*	Age	Gender (M/F)	MMSE	CDR (0/0.5/1)	CDR Sum-of-boxes
1	a	OC	115	77.2 ± 8.4	34/81	29.1 ± 1.1	115/0/0	0 ± 0
		Mild AD	29	77.5 ± 6.5	6/23	22.1 ± 3.5*	0/0/29	5.52 ± 1.51*
	b	Incipient AD	29	78.8 ± 7.1	19/10	27.0 ± 1.6*	0/29/0	1.22 ± 0.32*
		Very mild AD	40	76.0 ± 6.3	18/22	25.2 ± 3.8*	0/40/0	3.05 ± 0.81*
	c	OC PIB-neg	35	73.7 ± 7.5	7/28	29.7 ± 0.3	35/0/0	0 ± 0
		OC PIB-pos	9	71.4 ± 7.5	2/7	29.3 ± 0.6	9/0/0	0 ± 0
2		OC	22	78.1 ± 2.2	0/23	29.3 ± 0.8[a]	22/0/0	
		Mild AD	17	78.9 ± 3.7	5/12	21.5 ± 3.9*[a]	0/10/7	
3		OC	29	70.3 ± 6.6	12/17	29.4 ± 0.9	28/0/0	
		Mild AD	12	71.0 ± 8.9	8/4	24.6 ± 2.8*	0/2/10	
4		OC	28	74.3 ± 5.6	10/18	29.6 ± 0.5	28/0/0	
		Mild AD	15	78.3 ± 6.9	7/8	23.3 ± 4.2*	0/0/15	

Note: Values represent mean ± standard deviation. *$P < 0.001$ (different from OC). BDS-IMC = Blessed Dementia Score Information-memory-concentration.
[a]MMSE scores calculated from Blessed IMC scores (Thal et al. 1986).

et al. 1988, 2001; Morris 1993; Berg et al. 1998; Storandt et al. 2006). Many of these CDR = 0.5 individuals would be classified as having mild cognitive impairment in other settings (Morris et al. 2001; Storandt et al. 2006).

An additional 44 participants were asymptomatic normal OC (CDR = 0, MMSE 26–30) and had both amyloid-PIB PET data available (see below) as well as MRI data—this was Sample 1c.

Multiple (3 or 4) high-resolution structural T_1-weighted magnetization-prepared rapid gradient echo (MP-RAGE) images were acquired on a 1.5T Siemens Vision scanner (Siemens Medical Systems, Erlingan, Germany) with the following parameters: repetition time (TR) 9.7 ms, echo time (TE) 4 ms, flip angle (FA) 10, inversion time (TI) 20 ms, voxel size 1 × 1 × 1.25 mm. These data have been made openly available to the community (http://www.oasis-brains.org/).

Additional Participant Samples

Data from 3 additional samples of nondemented OC participants and AD patients were analyzed as part of this study. The 3 samples were drawn from separate ongoing studies at Massachusetts General Hospital, all of which were approved and conducted in accordance with guidelines established by the Partners Human Research Committee. Written informed consent was obtained from each participant, and from a caregiver for patients with AD with significant cognitive impairment. See Table 1 for detailed demographic and clinical data on these additional samples.

Assessments were conducted in a manner nearly identical to that described above (details have been previously published as cited below), with 39 participants in Sample 2 (Atri et al. 2005), 41 participants in Sample 3 (Wright, Dickerson, et al. 2007; Wright, Feczko, et al. 2007), and 40 participants in Sample 4 (Dickerson et al. 2005; Celone et al. 2006). The characteristics of the AD dementia participants in these samples were as follows; see also Table 1. In Sample 2, AD dementia participants had CDR = 0.5 ($N = 10$) or CDR = 1 ($N = 7$); mean MMSE = 21.5 (SD = 3.9), range 12–29. In Sample 3, AD participants had

were thinner in AD than OC, as illustrated in Figure 2. Regions of significant thinning were primarily located in limbic and heteromodal association areas, including rostral medial temporal, inferior temporal, temporal pole, precuneus, inferior parietal (supramarginal and angular gyri), superior parietal, inferior frontal, and superior frontal cortex. There were minor differences in the spatial location of regional thinning across hemispheres, but generally the regions were quite consistent bilaterally. Primary sensorimotor regions were largely spared.

Quantitative Analysis of Cortical Regions Vulnerable to AD

We next investigated the magnitude of AD-related thinning within each cortical region identified in the exploratory analysis. Cortical ROI label locations and group mean and standard error data are shown in Figure 3. Data for Sample 1a is shown in the leftmost pair of bars in each graph in Figure 3. Mean thickness, standard deviation, magnitude of group differences (in mm), percent thinning in AD compared with controls, and Cohen's *d* effect sizes are shown in Table 2.

Thinning due to AD was most prominent (in mm) in the rostral medial temporal cortex, with a mean magnitude of thinning of more than 0.4 mm (14% thinning in AD compared with OC). Other regions with more than 0.2 mm thinning included inferior temporal, temporal pole, inferior parietal (both angular and supramarginal gyri), and superior frontal regions, which ranged from 8.1% to 11.6% thinner in AD than OC. The regions with a relatively smaller magnitude of thinning (0.16–0.19 mm, or 7–8%) included precuneus, inferior frontal, and superior parietal regions. There was no significant thinning in the primary visual cortex (0.03 mm [2.2%], $P = 0.19$).

Consistency of Regional Cortical Thinning in Mild AD: Quantitative Analysis of Cortical Regions in 3 Separate Samples

The consistency of regionally specific cortical thinning was investigated in 3 additional samples of AD patients and OC individuals. This analysis was unbiased, as it employed cortical ROIs defined as above from Sample 1a and applied to separate samples of participants (by mapping each cortical ROI label from the average surface template to each individual via the spherical average surface, as described in Methods).

The magnitude of AD-related thinning within these cortical regions was remarkably consistent across the 3 additional samples. Figure 3 illustrates the mean thickness and standard error within regions across all 4 samples. Table 3 provides details of measurements from Samples 2, 3, and 4, showing magnitude of group difference (AD vs. OC), percent thinning in AD, and effect sizes.

Again, across all 3 additional samples, the medial temporal cortex showed the largest magnitude of thinning of all regions within each sample, ranging from 0.26 to 0.55 mm thinner in AD than OC. Temporal pole and inferior parietal regions showed consistently large effects, whereas inferior temporal, superior parietal, precuneus, and frontal regions were somewhat less consistent with respect to magnitude of thinning. Primary visual cortex again showed no effects in these 3 samples.

An additional analysis was performed to investigate thickness differences between the 4 samples. A main effect was found for Sample 2, with mean cortical thickness biased toward slightly thinner estimates without an interaction with diagnostic group.

Detection of Attenuated Regional Cortical Thinning in Individuals with Milder Symptoms of AD

We next investigated a sample (Sample 1b) of individuals with milder symptoms of AD to determine whether a lesser magnitude of cortical thinning would be detectable within regions known to be vulnerable to AD from the analyses above. All of these participants had an overall CDR rating of 0.5, but some were diagnosed with very mild AD ($n = 40$) and others were diagnosed with incipient AD ($n = 29$). See Table 1 for demographic and clinical data on these participants. The AD-signature cortical ROI labels, as defined from Sample 1a, were again applied to this sample of individuals with very mild AD or incipient AD.

AD-related thinning was detected within these cortical regions in a remarkably consistent manner across the 2 milder groups. Most of the regions demonstrated a pattern suggestive of progressive thinning across the 4 groups, as illustrated in Figure 4. The primary visual cortex showed no such effect. As depicted in Table 4, statistical analysis demonstrated that the all regions except the primary visual cortex were thinner in the very mild AD group than OC. Inspection of the percent thinning in very mild AD reveals a lesser degree of thinning in all regions than in the mild AD group. The magnitude of thinning in the incipient AD group is relatively small in all regions, with most differences in regional thickness compared with OC not reaching statistical significance (except angular and supramarginal gyri). The primary visual cortex ROI shows

Table 2
Quantitative metrics of thinning by region within sample #1

Region	Mean thickness (mm) (SD)				Group mean	Percent	Effect size
	OC		Mild AD		Difference (mm)	Thinning	
Medial temporal	2.91	(0.33)	2.51	(0.32)	0.40	13.62	1.22
Inferior temporal	2.67	(0.23)	2.36	(0.23)	0.31	11.46	1.33
Temporal pole	2.63	(0.21)	2.39	(0.20)	0.25	9.31	1.20
Angular	2.32	(0.16)	2.10	(0.24)	0.22	9.60	1.09
Superior frontal	2.55	(0.17)	2.35	(0.22)	0.20	7.83	1.02
Superior parietal	2.02	(0.13)	1.87	(0.14)	0.15	7.51	1.12
Supramarginal	2.38	(0.17)	2.18	(0.20)	0.20	8.43	1.08
Precuneus	2.21	(0.18)	2.03	(0.18)	0.18	8.07	0.99
Inferior frontal	2.16	(0.13)	2.01	(0.15)	0.15	6.96	1.07
Primary visual	1.51	(0.12)	1.48	(0.14)	0.03	2.29	0.27

Note: Effect size = Cohen's *d* effect size. All regions are significantly thinner in AD than OC ($P < 0.01$) except for primary visual, which is not statistically different between OC and AD groups.

Table 3
Quantitative metrics of thinning by region within 3 additional samples of participants

Region	Mean difference (mm)			Percent thinning			Effect size		
Sample	2	3	4	2	3	4	2	3	4
Medial temporal	0.38***	0.36***	0.55***	13.00	12.06	18.68	1.40	1.38	1.54
Inferior temporal	0.14	0.25***	0.10	5.46	9.19	4.08	0.50	1.48	0.41
Temporal pole	0.31***	0.22*	0.32***	12.36	8.03	11.88	1.17	0.93	1.55
Angular	0.09	0.27***	0.21***	4.20	11.91	9.25	0.54	1.42	1.25
Superior frontal	0.11	0.19**	0.32***	4.75	8.03	12.96	0.45	0.98	1.45
Superior parietal	0.18**	0.08	0.08*	10.01	4.20	3.98	1.07	0.41	0.68
Supramarginal	0.20**	0.23**	0.16*	9.18	10.04	6.80	1.09	1.05	0.84
Precuneus	0.10	0.18*	0.16*	5.08	8.40	7.21	0.51	0.97	0.74
Inferior frontal	0.14*	0.13*	0.15***	6.75	5.98	7.10	0.85	0.91	1.16
Primary visual	0.06	0.00	0.03	4.62	0.16	2.28	0.61	0.02	0.25

Note: Effect size = Cohen's *d* effect size. Regions of significant thinning in AD as compared with OC (*$P < 0.05$; **$P < 0.005$; ***$P < 0.001$).

Table 4
Quantitative metrics of thinning by region within incipient and very mild AD participants

Region	Mean thickness (mm) (SD)						Percent thinning (vs. OC)		Effect Size (vs. OC)	
	OC		Incipient AD		Very mild AD		Incipient AD	Very mild AD	Incipient AD	Very mild AD
Medial temporal	2.91	(0.33)	2.80	(0.30)	2.63	(0.37)	$3.89^{V,A}$	$9.65^{C,I}$	0.36	0.80
Inferior temporal	2.67	(0.23)	2.62	(0.23)	2.53	(0.20)	1.69^{A}	$4.97^{C,A}$	0.19	0.60
Temporal pole	2.63	(0.21)	2.55	(0.24)	2.52	(0.21)	3.14^{A}	$4.39^{C,A}$	0.37	0.55
Angular	2.32	(0.16)	2.21	(0.18)	2.16	(0.14)	$4.46^{C,A}$	6.39^{C}	0.61	1.06
Superior frontal	2.55	(0.17)	2.49	(0.20)	2.43	(0.19)	2.29^{A}	4.84^{C}	0.31	0.67
Superior parietal	2.02	(0.13)	1.98	(0.18)	1.92	(0.13)	2.08^{A}	5.12^{C}	0.27	0.80
Supramarginal	2.38	(0.17)	2.28	(0.18)	2.26	(0.18)	$3.88^{C,A}$	4.89^{C}	0.53	0.67
Precuneus	2.21	(0.18)	2.15	(0.28)	2.08	(0.22)	2.43^{A}	5.84^{C}	0.23	0.64
Inferior frontal	2.16	(0.13)	2.14	(0.14)	2.03	(0.19)	$1.15^{V,A}$	$6.28^{C,I}$	0.19	0.85
Primary visual	1.51	(0.12)	1.52	(0.16)	1.50	(0.12)	0.39	0.89	0.04	0.11

Note: Superscripts indicate that the group is significantly different from OC (C), incipient AD (I), very mild AD (V), or mild AD (A) ($P < 0.05$, uncorrected). Percent thinning is in comparison to OC group (data presented in Table 3). Effect size is Cohen's *d*.

a remarkable degree of reliability with respect to absolute cortical thickness across the groups (lower right graph in Fig. 4). Figure 4 illustrates the mean thickness and standard error within regions across the very mild AD and incipient AD groups, with the OC and mild AD groups shown for comparison. Table 4 provides details of measurements from these 2 groups of participants.

Relationship of Regional Cortical Thinning to Severity of Clinical Impairment

We analyzed the relationship of the regional measures of cortical thickness to severity of symptoms of cognitive impairment within all the demented participants from Washington University (incipient AD, very mild AD, mild AD; $N = 97$). Correlational analyses were run with the CDR Sum-of-Boxes (CDR-SB) as the dependent measure. Although the overall CDR ratings (0.5 or 1) of these individuals indicated that they were very mildly or mildly demented, the CDR-SB provides a finer grading of impairment within this spectrum, ranging in this sample of 97 participants between 0.5 and 9.0. CDR-SB was inversely correlated with the thickness of a number of regions, including medial temporal, inferior temporal, temporal pole, angular gyrus, superior parietal, superior frontal, and inferior frontal cortex (Pearson R values ranging from –0.24 through –0.38, all P values < 0.02). These findings indicate that a greater level of clinical impairment is associated with a larger magnitude of thinning within these cortical regions. A stepwise multiple linear regression analysis was performed with each of these regions as independent variables and CDR-SB as the dependent variable. This model indicated that a linear combination of medial temporal, inferior temporal, and inferior frontal regions was the best predictor of CDR-SB ($R = 0.51$, $F_{3,93} = 11.2$, $P < 0.001$).

These correlative analyses with CDR-SB were also examined within the diagnostic groups. The mild AD group demonstrated trends for superior ($R = –0.35$, $P = 0.06$) and inferior frontal ($R = –0.32$, $P = 0.08$) regions, whereas the very mild AD group demonstrated an effect for the medial temporal cortex ($R = –0.34$, $P = 0.03$) and a trend for the angular gyrus ($R = –0.28$, $P = 0.08$). There were no effects in the incipient AD group.

Pooled Multicenter Mapping Analysis of the Magnitude of Cortical Thinning in Mild AD

For this analysis, a general linear model was constructed that included all 4 mild AD and all 4 OC groups. Each participant contributed a cortical thickness estimate mapped to the group using spherical registration. The contrast of interest was AD versus OC, and was weighted according to the number of participants in each group. The parameter estimate of difference in cortical thickness between AD and OC was then used to generate a map of the magnitude of cortical thinning in AD. Note that this map is quantitative revealing the estimated size (in mm) of cortical thinning. Thus, this map reflects our best estimate of the topography and magnitude of cortical thinning in mild AD.

Figure 5 illustrates the results of the pooled analysis, which was undertaken to map the magnitude of thinning across the entire cerebral cortex in Samples 1a, 2, 3, and 4 comparing AD with OC (total $N = 267$). Areas of the cortex in which the magnitude of AD-related thinning exceeds 0.15 mm are shown, using a color scale to indicate the magnitude of thinning. The spatial topography of regional thinning parallels that illustrated with the statistical map of Sample 1a alone (Fig. 2). The areas with the greatest magnitude of thinning across this large multicenter dataset, such as medial temporal cortex, are quite similar to those indicated by the ROI analyses of thinning within each sample above. The congruence of the effects detected with this pooled analysis and those detected above using hypothesis-driven replication samples supports the feasibility of pooled analyses of cortical thickness in multisite/multiscanner data using the high-throughput computational analysis system. A Supplementary Table provides the estimates of the magnitude of thinning in AD for the entire pooled sample.

Detection of Regional Cortical Thinning in Amyloid-Positive Asymptomatic Older Individuals

We next investigated a sample (Sample 1c) of individuals evaluated in the same fashion as that described above for Sample 1a, and who were considered to be asymptomatic OC (CDR = 0). Based on PIB-PET scans, they were dichotomized into OC participants with (amyloid-positive, $N = 9$) or without (amyloid-negative, $N = 35$) PIB amyloid binding. We sought to determine whether subtle cortical thinning might be detectable within regions known to be vulnerable to AD from the analyses above. See Table 1 for demographic and clinical data on these participants. The AD-signature cortical ROI labels, as defined from Sample 1a, were again applied to this sample of amyloid-positive or amyloid-negative OC individuals.

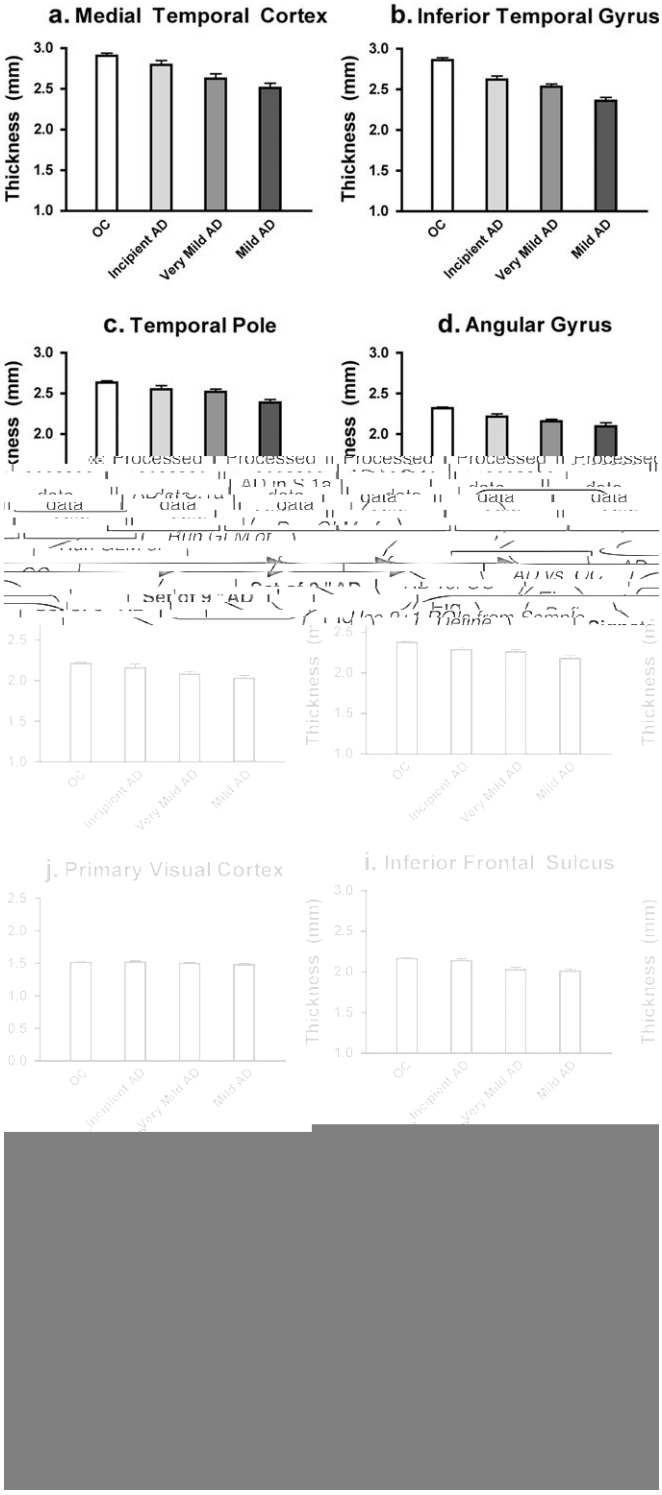

Figure 4. Thinning in cortical ROIs in incipient and very mild AD participants. ROIs were generated from exploratory analysis in subject Sample 1a (see Fig. 2, same ROIs as used in Fig. 3) and applied to a new sample of Incipient and very mild AD patients (CDR = 0.5, Sample 1b) to test the hypothesis that these regions are thinner in the mildest clinical stages of AD than controls. Graphs show mean cortical thickness within each ROI across the 2 mildly impaired samples, in comparison to controls and mildly impaired (CDR = 1) AD patients (Sample 1a). A primary visual cortex region was also used to illustrate minimal effects on this region (lower right). Error bars indicate 1 standard error of the mean. See Table 3 for statistics. (*A*) Medial temporal cortex, (*B*) Inferior temporal gyrus, (*C*) Temporal pole, (*D*) Angular Gyrus, (*E*) Superior frontal gyrus, (*F*) Superior parietal lobule, (*G*) Supramarginal gyrus, (*H*) Precunes, (*I*) Inferior frontal sulcus, (*J*) Primary visual cortex.

AD-related thinning was detected within the temporal pole (5.8% thinning, $P = 0.04$) and a trend was present in the superior frontal cortex (4.6% thinning, $P = 0.06$) in the amyloid-positive OC group compared with the amyloid-negative OC group. Most other regions demonstrated a pattern suggestive of subtle thinning (see Fig. 7), but the small sample size lacked power for statistical demonstration of effects. Thus, the thickness measures from all 9 ROIs were averaged to create a single mean "AD cortical signature" thickness measure. A trend toward thinning in this mean AD cortical signature measure was present in the amyloid-positive OC group compared with the amyloid-negative OC group ($P = 0.09$). This finding was further supported by a post hoc comparison that demonstrated thinning in the mean AD cortical signature measure of the amyloid-positive OC group compared with the larger OC (amyloid status unknown, $N = 115$) group from Sample 1a ($P < 0.05$). Mean thickness of the entire cortex in the amyloid-positive group (2.17 ± 0.11 mm) did not differ from that of the amyloid-negative group (2.13 ± 0.7 mm) nor from that of the larger OC group from Sample 1a (all P values > 0.19). Figure 6 illustrates the AD cortical signature measure (mean and standard error of the mean) across the amyloid-positive OC, amyloid-negative OC, and other 4 groups from Samples 1a, 1b, and 1c.

Discussion

The pathology of AD typically has a predilection for limbic allocortical and heteromodal association neocortical areas (Brun and Gustafson 1976; Arnold et al. 1991; Braak and Braak 1991). Quantitative analysis of MRI has been used to identify, in living AD patients, abnormalities in the normal anatomic properties—such as volume, gray matter density, and thickness—of the cerebral cortex using manual a priori ROI-based MRI techniques (Jack et al. 1997; Juottonen et al. 1998; Bobinski et al. 1999; Killiany et al. 2000; Dickerson et al. 2001) and more recently using semiautomated exploratory mapping techniques (Baron et al. 2001; Thompson et al. 2001; Good et al. 2002; Scahill et al. 2002; Karas et al. 2003; Buckner et al. 2005; Lerch et al. 2005; Du et al. 2007; Whitwell et al. 2008). In the present work, we pursued a novel approach combining exploratory mapping and a priori ROI-based measurement techniques, first by performing an exploratory analysis of cortical thickness across the entire cortical mantle to map the "cortical signature" of regional thinning in mild AD and then by using this map to generate ROIs to measure, in an a priori fashion, the consistency of regional cortical thinning in multiple independent samples of mild AD patients and the presence of thinning in milder forms of AD.

These additional analyses revealed a lesser magnitude of thinning in patient groups with milder symptoms of AD consistent with mild cognitive impairment (Morris et al. 2001; Storandt et al. 2002, 2006). Even within AD patients spanning the circumscribed spectrum of incipient, very mild, and mild AD, the thickness of many of the critical cortical regions correlates with the relative severity of clinical impairments. Of particular interest, a very mild degree of cortical thinning in these regions was detected in amyloid-positive OC (CDR = 0) individuals, indicating that subtle anatomic change in a pattern consistent with AD begins to occur in asymptomatic individuals who harbor AD pathology. To provide a stable estimate of cortical thinning in AD, Figure 5 maps a pooled analysis of the

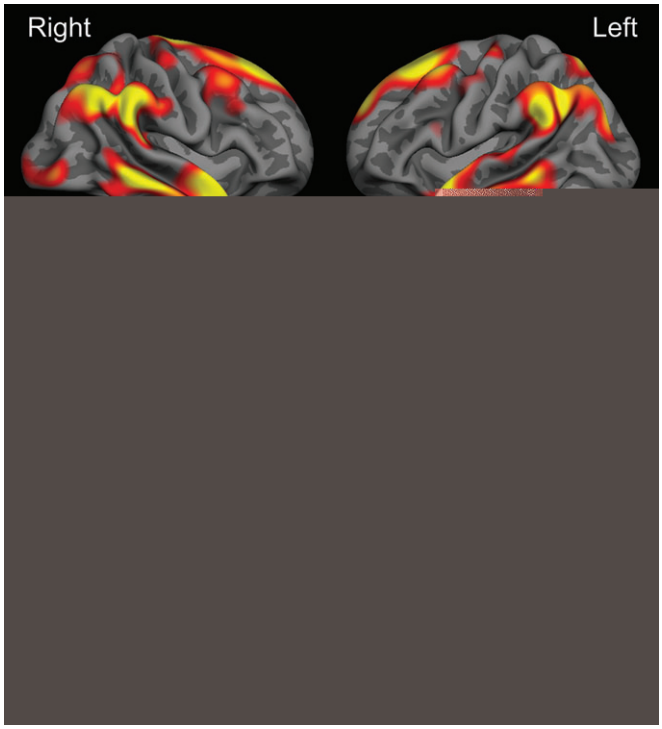

Figure 5. Magnitude of cortical thinning in AD in millimeters, derived from pooled analysis of 4 samples of participants (Samples 1a, 2, 3, and 4). Map shows parameter estimate of amount of thinning across cerebral cortex from general linear model analysis of 267 participants, showing areas where cortex is at least 0.15 mm thinner in AD group than OC group. Color scale shows magnitude of thinning from 0.15 mm (red) through 0.2 mm (yellow) in AD compared with OC.

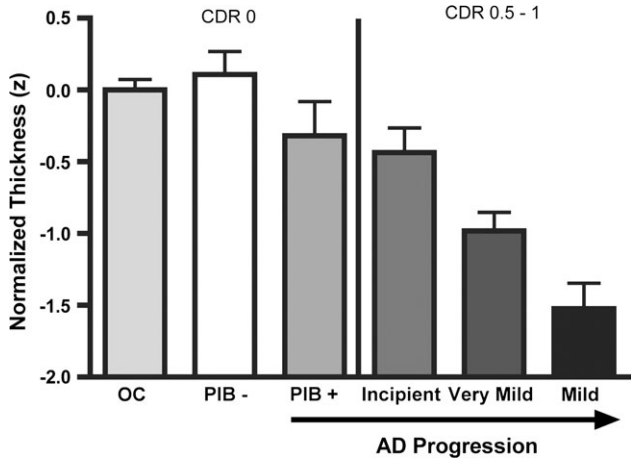

Figure 6. Mean thickness of AD cortical signature regions is decreased in amyloid (PIB)-positive OC (CDR = 0), and demonstrates progressive thinning as the symptoms of AD dementia become progressively more prominent across the spectrum of Incipient, very mild, and mild AD dementia. Bars represent mean thickness of the 9 cortical regions shown in Figure 2, normalized for age and standardized to *Z* scores (*y* axis). Error bars indicate 1 standard error of the mean. The leftmost 3 groups are all OC (CDR = 0, MMSE 25–30), ordered by PIB status unknown (unk) ($N = 115$), PIB negative ($N = 35$), and PIB positive ($N = 9$). The rightmost 3 groups are all PIB status unknown, but are progressively more impaired with clinical symptoms ranging from incipient AD (CDR = 0.5/CDR-SB = 1.2, $N = 29$), very mild AD (CDR = 0.5/CDR-SB = 3.5, $N = 40$), and mild AD (CDR = 1/CDR-SB = 5.5, $N = 29$). Figure includes data from Samples 1a, 1b, and 1c.

magnitude of cortical thinning in all 76 mild AD patients compared with all 194 OC participants from the 4 samples.

Taken collectively, these observations show that this high-throughput, semiautomated MRI data analysis procedure for quantifying cortical thickness is feasible for pooled analysis of multisite data, such as is typical for clinical trials or other large multicenter studies. The method is sensitive enough to detect subtle changes in cortical regions specifically affected by AD prior to the onset of even the mildest symptoms.

AD-Related Regional Thinning Parallels the Topography of Neuropathology

The spatial topography of cortical thinning in AD that we observed in vivo in the present study is consistent with the spatial distribution of neurodegenerative change known to occur in the disease from post-mortem studies (Brun and Gustafson 1976; Arnold et al. 1991; Braak and Braak 1991) and from recent in vivo PET investigations using tracers that bind to pathologic proteins (Klunk et al. 2004; Buckner et al. 2005; Mintun et al. 2006; Small et al. 2006). These regions also represent the major limbic and heteromodal cortical areas (Mesulam 1998).

The spatial topography of regional cortical thinning that we identified in mild AD is consistent with previous observations using voxel-based morphometry (Baron et al. 2001; Karas et al. 2003; Bozzali et al. 2006; Whitwell et al. 2008) and similar techniques (Thompson et al. 2001; Scahill et al. 2002; Buckner et al. 2005; Apostolova et al. 2007) as well as 2 previous investigations using cortical thickness techniques (Lerch et al. 2005; Du et al. 2007). Generally, these efforts have converged upon a similar pattern of atrophy that is present in the medial temporal, lateral temporoparietal, and midline parietal regions, with variable findings in frontal regions. The major contribution of the present work relates to the demonstration of a consistent, stable estimate of the localization of relatively prominent cortical thinning in a large multicenter sample of mild AD patients, which can be used to predict the presence of thinning in milder and presymptomatic patient groups.

The magnitude of thinning within some regions is relatively large given the patients' mild level of dementia—even at early clinical stages of the illness, several regions are 10–20% thinner than normal. The regions with a larger degree of thinning—medial temporal, inferior temporal, temporal pole, inferior parietal, and posterior cingulate/precuneus—are those typically thought to be affected earliest in the course of the disease on the basis of the burden of pathologic accumulation (Hyman et al. 1984; Van Hoesen et al. 1986; Arnold et al. 1991; Arriagada, Growdon, et al. 1992; Arriagada, Marzloff, et al. 1992), neuronal loss, and gliosis (Brun and Gustafson 1976). A number of previous studies of cortical atrophy in AD have focused on spatial localization but have not estimated the magnitude of effects (Baron et al. 2001; Frisoni et al. 2002; Scahill et al. 2002; Buckner et al. 2005). Estimates of the magnitude of cortical atrophy have demonstrated the largest effects in temporal and parietal cortex (Karas et al. 2004; Du et al. 2007), with 15–20% thinning in caudal lateral temporal and posterior parietal cortex (Thompson et al. 2001, 2003; Lerch et al. 2005; Apostolova et al. 2007) as well as medial temporal cortex (Lerch et al. 2005). The results of the present study are quite consistent with these previous studies, and contribute by showing that similar but milder effects are present in patients with clinically milder forms of AD.

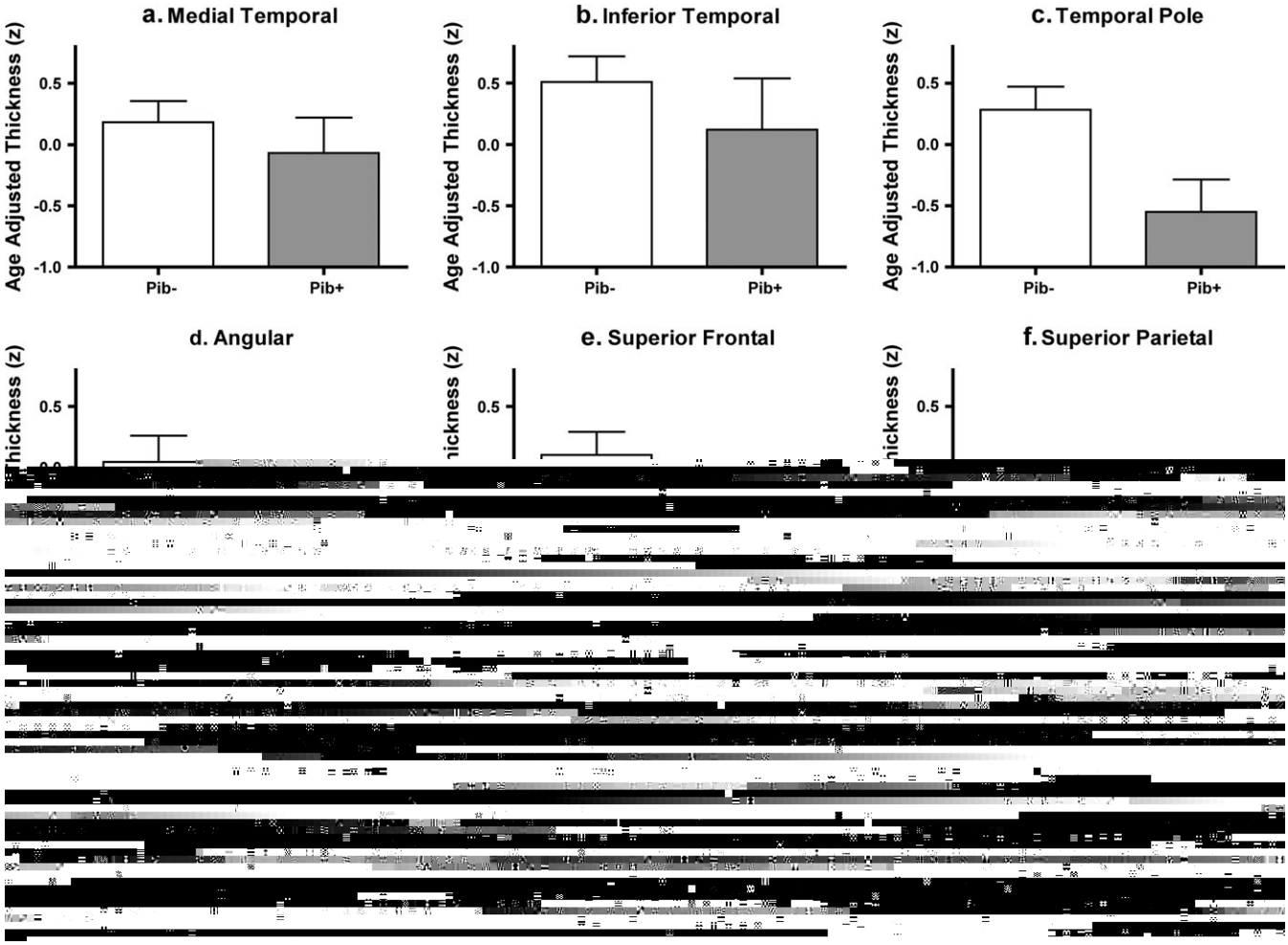

Figure 7. Consistent subtle thinning appears to be present in many cortical ROIs in amyloid (PIB)-positive OC (CDR = 0) compared with amyloid (PIB)–negative controls. ROIs were generated from exploratory analysis in subject Sample 1a (see Fig. 2, same ROIs as used in Fig. 3) and applied to a new sample of PIBþ and PIB- controls (CDR = 0, Sample 1c) to test the hypothesis that these regions undergo subtle thinning in asymptomatic AD. Bars represent mean thickness of each region shown in Figure 2, normalized for age and standardized to *Z* scores. Error bars indicate 1 standard error of the mean. (*A*) Medial temporal cortex, (*B*) Inferior temporal gyrus, (*C*) Temporal pole, (*D*) Angular Gyrus, (*E*) Superior frontal gyrus, (*F*) Superior parietal lobule, (*G*) Supramarginal gyrus, (*H*) Precunes, (*I*) Inferior frontal sulcus.

MRI Measures of Regional Cortical Thinning in AD Correlate with Severity of Symptoms of the Disease

Previous studies have shown that AD-related thinning of particular cortical regions correlates with worse performance on cognitive testing in patients spanning a relatively broad spectrum of clinical impairment, including a sizable number of moderately demented patients (Lerch et al. 2005; Du et al. 2007). In the present study, we specifically focused on the relatively narrow clinical spectrum of incipient, very mild, and mild AD, and investigated the relationship of regional cortical thickness to CDR-SB. The CDR-SB is a finely graded measure that reflects the clinician's impression of the relative severity of cognitive symptoms that affect memory, orientation, judgment, and problem-solving, and daily function at home and in the community. It is widely used in clinical research, including trials of putative therapeutic agents. The CDR-SB is strongly associated with cortical thickness in many of the regions identified in this study, suggesting that progressive worsening of cognitive impairment within the very mild to mild spectrum of AD is associated with progressive thinning of specific heteromodal regions of the cortex. Because the CDR-SB is a clinical measure of impairment primarily reflecting symptom severity in daily life, our results support the clinical validity of regional cortical thickness measures as an imaging biomarker of AD severity.

Although the data in this study are cross-sectional, inferences can be made regarding the sequence of involvement of the cortical regions in the course of AD. Based on the analysis comparing the 4 groups of participants from Sample 1a and 1b, some regions, particularly ventromedial temporal and inferior parietal cortex, exhibit thinning even in the mildest (incipient AD) group, suggesting very early involvement. Other regions, particularly superior parietal and frontal cortex, do not show appreciable thinning until symptoms are more prominent (very mild to mild AD dementia), suggesting that they become involved later in the course of the disease (Scahill et al. 2002; Buckner et al. 2005). Similarly, from the within-group correlational analyses, symptom severity (CDR-SB) within the very mild AD patient group correlates with medial temporal and inferior parietal thinning, whereas symptom severity within the mild AD patient group correlates with thinning in frontal regions, again suggesting temporoparietal involvement prior to frontal involvement. These inferences are consistent with those made from pathologic studies (Arriagada, Marzloff, et al. 1992;

Braak et al. 1998), but longitudinal MRI data will be required for confirmation.

Detection of cortical thinning in asymptomatic amyloid-positive individuals

The development of technology to image fibrillar amyloid deposits in living individuals (Klunk et al. 2004) has led to the confirmation of findings from post-mortem studies (Tomlinson et al. 1968; Price et al. 1991; Bennett et al. 2006) that amyloid pathology may be present in some cognitive intact older individuals (Buckner et al. 2005; Mintun et al. 2006). The topographic distribution of amyloid in the neocortex appears to overlap in many respects that of atrophy in AD (Buckner et al. 2005).

We demonstrate here that subtle thinning is present in some AD cortical signature ROIs in a group of asymptomatic OC individuals who are amyloid-positive (Fig. 6). An aggregate measure of the thickness of the AD cortical signature regions in these asymptomatic older individuals revealed subtle thinning in comparison to the large group (N = 115) of OC individuals from Sample no. 1 whose amyloid status is unknown. The ability to detect thinning in these cortical regions in asymptomatic amyloid-positive individuals suggests that the approach to regional cortical thickness measurement outlined here may be useful as a biomarker of early disease, and it will be of great interest to follow such individuals longitudinally with both imaging and clinical assessments. It will also be important to demonstrate whether this putative imaging biomarker has reasonable sensitivity and specificity at the individual subject level.

Regional Cortical Thinning in Mild AD is Consistent across 4 Patient Samples

The consistency of regional cortical thinning across the 4 samples of mild AD patients is remarkable, despite a variety of sample- and instrument-related factors that could have contributed to variability. Sample-related factors that could increase variability of cortical thinning in AD include severity of clinical impairment, which in this study is relatively similar across the samples based on CDR and mental status test scores (yet these clinical measures themselves are associated with a certain level of unreliability across sites). Because diagnoses have been made clinically, the probable inclusion of some individuals in each sample with other pathologies in addition to (or instead of) AD could also increase variability of cortical thickness measures. Moreover, variability in cortical thickness across normal participants as well as AD patients can be influenced by age and sex (Salat et al. 2004), which do differ in these samples and although controlled for statistically may still have exerted subtle influence. Finally, and potentially most importantly, MRI instrument-related factors may contribute to variability, including scanner model, head coil, pulse sequence, and field strength. Across the 4 samples, the scanners were all made by the same manufacturer and employed versions of the same sequence, but the scanner models, head coils, and software operating systems differed, and one sample was scanned at 3.0 Tesla, whereas the others were scanned at 1.5 Tesla. Yet the variability in cortical thickness measures across the samples was remarkably low, as illustrated by the medial temporal cortex, the thickness of which ranged between 2.9 and 3.0 mm in the control groups of all 4 samples (Fig. 3, upper left graph). Variability within a single sample appears even lower, as can be seen by examining the primary visual cortex measure in the Washington University sample across the 4 clinical groups, which is centered almost exactly on 1.5 mm (Fig. 4, lower right graph). There are some regions in which variability of thinning across samples is higher, particularly superior parietal and inferior temporal, the origins of which are unclear but may relate to differences in the clinical characteristics of the samples, or to heterogeneity of levels of pathology. Further studies of the contributors to variability in cortical thickness estimates will be useful to better understand the potential effects of factors that did not vary in this study, such as scanner manufacturer or sequence (Han et al. 2006; Dickerson et al. 2008).

The consistency of AD-related cortical thinning across the multiple subject samples strongly supports the notion that pooling of multisite MRI data is feasible for cortical thickness analysis (Mueller et al. 2005; Murphy et al. 2006). Further support for this point is presented in Figure 5, which illustrates the cortical map derived from a combined analysis of the 267 participants in all 4 mildly impaired (CDR = 1) samples. Regions in which the thickness of the cerebral cortex of AD patients is at least 0.15 mm thinner than OC are graded in terms of degree of thinning. This map illustrates the spatial topography of the effects quantified in Tables 3 and 4, showing that medial temporal cortex has the greatest magnitude of thinning, followed by temporal pole, inferior temporal, and inferior parietal cortex. Because it encompasses a large number of participants drawn from multiple samples, we believe it is the best current estimate of the degree of regional cortical thinning in mild AD. The map in Figure 5 depicts a spatial distribution of thinning magnitude that is remarkably similar to the map in Figure 2, which shows the statistical significance of the general linear model comparing thickness in AD versus OC. Regions may differ between the 2 maps because of variance, with some regions with relatively prominent thinning showing lesser statistical effects because of greater variance (e.g., posterior cingulate). Comparison of these 2 maps again reinforces the point that pooled analysis of multiple samples of MRI data can be used to robustly detect disease-related effects.

Value of High-Throughput Automated MRI Data Analysis

The MRI data analysis procedure used here to quantify cortical thickness in the 380 scans in the present study is nearly fully automated, with manual operator involvement at a few key processing steps for checking and minor corrections to, for example, the skull stripping procedure. Thus, this high-throughput data analysis system will likely lend itself well to analyses of large data sets from clinical trials or studies such as the ADNI. The quantitative measures of the thickness of the AD cortical signature regions identified in this study can be derived for individual participants and compared with a control group to assist in diagnosis or to establish a baseline for longitudinal comparison.

An important aspect of the analytic approach used in this study is that the ROIs were localized based on an exploratory analysis of the "disease effect" of AD across the entire cortical mantle without the use of a priori constraints tied to particular anatomic features of the cortex. That is, the ROIs were not delimited based on gyral crowns, sulcal fundi, or other elements of cortical folding patterns often used to demarcate cortical ROIs. The generation of "disease localizer" ROIs from an initial exploratory analysis, followed by the use of such localizers to test hypotheses in separate participant samples, is

analogous to the use of "functional localizers" in functional neuroimaging studies. Just as functionally specific cortical regions may not obey the constraints of cortical folding patterns (Eickhoff et al. 2006), neurodegenerative diseases may selectively affect subregions within larger traditional anatomic regions (e.g., precuneus), or may traverse the gyral or sulcal boundaries of ROIs defined using such landmarks.

Although a strength of the present study is its focus on mild clinical stages of AD, important limitations include the lack of longitudinal data and that the clinical diagnosis of AD is not supported by other imaging markers or by autopsy. It will be important to perform retrospective analyses of MRI data from individuals who have been demonstrated by autopsy to have definite AD with a typical pattern of pathology. It will also be of great interest to perform multimodal in vivo studies combining MRI measures of cortical thickness with imaging markers of pathology (Buckner et al. 2005). It is possible that in vivo pathologic markers may indicate, with a high degree of specificity, which individuals harbor AD pathology, but that MRI-derived measures of cortical thinning may be sensitive predictors of the emergence of clinical symptoms, but this hypothesis will require focused investigation.

Possible Biological Contributors to Cortical Thinning in AD

Studies of post-mortem tissue have shown that thickness is reduced in regions of the cerebral cortex that are affected pathologically in AD (Gomez-Isla et al. 1996; Regeur 2000). Although a few investigations have demonstrated that MRI-derived hippocampal volume correlates with neurofibrillary tangle burden in AD patients (Gosche et al. 2002; Jack et al. 2002; Silbert et al. 2003; Csernansky et al. 2004), the histologic determinants of cortical thinning are unknown. Some regions with prominent thinning identified in the present study are primarily affected by neurofibrillary tangles early in the course of the disease and to a much lesser degree by plaques (e.g., medial temporal cortex), whereas others carry a heavy burden of both major pathologic markers of AD (e.g., temporal pole and rostral inferior temporal gyrus) (Brun and Gustafson 1976; Arnold et al. 1991; Braak and Braak 1991; Arriagada, Marzloff, et al. 1992). It is notable that regions in which amyloid deposition tends to be prominent from PIB imaging data (prefrontal, gyrus rectus, precuneus, lateral temporal) are not areas in which prominent thinning is found. Although cortical thinning may be an indicator of the burden of neurofibrillary tangles, neuritic plaques, or other pathology, it is likely a more global indicator of the disruption of the healthy anatomic configuration of the cortical mantle. This may be a sign of the loss of neuronal, glial, or other important cellular components such as neuropil volume, which reflects synaptic numbers and extent of dendritic branching, both of which are markedly reduced early in the course of AD (Coleman and Flood 1987; DeKosky and Scheff 1990; Scheff et al. 1990; DeKosky et al. 1996; Coleman et al. 2004) and relate to degree of cognitive impairment (Terry et al. 1991). Higher-resolution MRI data (Schleicher et al. 2005) will probably be required to test hypotheses (Arnold et al. 1991) about laminar-specific patterns of abnormalities in AD and related disorders.

Supplementary Material

Supplementary material can be found at: http://www.cercor.oxfordjournals.org/

Funding

National Institute on Aging grants (K23-AG22509, P50-AG05134, P50-AG05681, and P01-AG03991, R01-AG29411, R21-AG29840); National Institute of Neurological Disorders and Stroke grants (R01-NS042861, National Center for Research Resources P41-RR14075, U24-RR021382); the Alzheimer's Association; Howard Hughes Medical Institute; and the Mental Illness and Neuroscience Discovery Institute.

Notes

We thank the faculty and staff of the Washington University ADRC, the Massachusetts ADRC, and the Memory Disorders Unit of Brigham and Women's Hospital. We thank the staff at the Martinos Center for Biomedical Imaging, particularly Mary Foley, Larry White, and Jill Clark, for their technical expertise. We express special appreciation to the participants in this study and their families for their valuable contributions, without which this research would not have been possible. *Conflict of Interest*: None declared.

Address correspondence to Brad Dickerson, MD, MGH Gerontology Research Unit, 149 13th St, Suite 2691, Charlestown, MA 02129, USA. Email: bradd@nmr.mgh.harvard.edu.

References

Apostolova LG, Steiner CA, Akopyan GG, Dutton RA, Hayashi KM, Toga AW, Cummings JL, Thompson PM. 2007. Three-dimensional gray matter atrophy mapping in mild cognitive impairment and mild Alzheimer disease. Arch Neurol. 64:1489–1495.

Arnold SE, Hyman BT, Flory J, Damasio AR, Van Hoesen GW. 1991. The topographical and neuroanatomical distribution of neurofibrillary tangles and neuritic plaques in the cerebral cortex of patients with Alzheimer's disease. Cereb Cortex. 1:103–116.

Arriagada PV, Growdon JH, Hedley-Whyte ET, Hyman BT. 1992. Neurofibrillary tangles but not senile plaques parallel duration and severity of Alzheimer's disease. Neurology. 42:631–639.

Arriagada PV, Marzloff K, Hyman BT. 1992. Distribution of Alzheimer-type pathologic changes in nondemented elderly individuals matches the pattern in Alzheimer's disease. Neurology. 42:1681–1688.

Atri A, Locascio JJ, Lin JM, Yap L, Dickerson BC, Grodstein F, Irizarry MC, Growdon JH, Greenberg SM. 2005. Prevalence and effects of lobar microhemorrhages in early-stage dementia. Neurodegener Dis. 2:305–312.

Baron JC, Chetelat G, Desgranges B, Perchey G, Landeau B, de la Sayette V, Eustache F. 2001. In vivo mapping of gray matter loss with voxel-based morphometry in mild Alzheimer's disease. Neuroimage. 14:298–309.

Bennett DA, Schneider JA, Arvanitakis Z, Kelly JF, Aggarwal NT, Shah RC, Wilson RS. 2006. Neuropathology of older persons without cognitive impairment from two community-based studies. Neurology. 66:1837–1844.

Berg L, McKeel DW, Jr, Miller JP, Storandt M, Rubin EH, Morris JC, Baty J, Coats M, Norton J, Goate AM, et al. 1998. Clinicopathologic studies in cognitively healthy aging and Alzheimer's disease: relation of histologic markers to dementia severity, age, sex, and apolipoprotein E genotype. Arch Neurol. 55:326–335.

Bobinski M, de Leon MJ, Convit A, De Santi S, Wegiel J, Tarshish CY, Saint Louis LA, Wisniewski HM. 1999. MRI of entorhinal cortex in mild Alzheimer's disease. Lancet. 353:38–40.

Bozzali M, Filippi M, Magnani G, Cercignani M, Franceschi M, Schiatti E, Castiglioni S, Mossini R, Falautano M, Scotti G, et al. 2006. The contribution of voxel-based morphometry in staging patients with mild cognitive impairment. Neurology. 67:453–460.

Braak H, Braak E. 1991. Neuropathological staging of Alzheimer-related changes. Acta Neuropathol (Berl). 82:239–259.

Braak H, Braak E, Bohl J, Bratzke H. 1998. Evolution of Alzheimer's disease related cortical lesions. J Neural Transm Suppl. 54:97–106.

Brun A, Gustafson L. 1976. Distribution of cerebral degeneration in Alzheimer's disease. A clinico-pathological study. Arch Psychiatr Nervenkr. 223:15–33.

Buckner RL, Head D, Parker J, Fotenos AF, Marcus D, Morris JC, Snyder AZ. 2004. A unified approach for morphometric and functional data analysis in young, old, and demented adults using automated atlas-based head size normalization: reliability and validation against manual measurement of total intracranial volume. Neuroimage. 23:724–738.

Buckner RL, Snyder AZ, Shannon BJ, LaRossa G, Sachs R, Fotenos AF, Sheline YI, Klunk WE, Mathis CA, Morris JC, et al. 2005. Molecular, structural, and functional characterization of Alzheimer's disease: evidence for a relationship between default activity, amyloid, and memory. J Neurosci. 25:7709–7717.

Cardenas VA, Du AT, Hardin D, Ezekiel F, Weber P, Jagust WJ, Chui HC, Schuff N, Weiner MW. 2003. Comparison of methods for measuring longitudinal brain change in cognitive impairment and dementia. Neurobiol Aging. 24:537–544.

Celone K, Calhoun V, Dickerson BC, Atri A, Chua E, Miller S, Depeau K, Rentz DM, Selkoe DJ, Blacker D, et al. 2006. Alterations in memory networks in mild cognitive impairment and Alzheimer's disease: an independent component analysis. J Neurosci. 26:10222–10231.

Coleman P, Federoff H, Kurlan R. 2004. A focus on the synapse for neuroprotection in Alzheimer disease and other dementias. Neurology. 63:1155–1162.

Coleman PD, Flood DG. 1987. Neuron numbers and dendritic extent in normal aging and Alzheimer's disease. Neurobiol Aging. 8:521–545.

Csernansky JG, Hamstra J, Wang L, McKeel D, Price JL, Gado M, Morris JC. 2004. Correlations between antemortem hippocampal volume and postmortem neuropathology in AD subjects. Alzheimer Dis Assoc Disord. 18:190–195.

Dale AM, Fischl B, Sereno MI. 1999. Cortical surface-based analysis. I. Segmentation and surface reconstruction. Neuroimage. 9:179–194.

DeKosky ST, Scheff SW. 1990. Synapse loss in frontal cortex biopsies in Alzheimer's disease: correlation with cognitive severity. Ann Neurol. 27:457–464.

DeKosky ST, Scheff SW, Styren SD. 1996. Structural correlates of cognition in dementia: quantification and assessment of synapse change. Neurodegeneration. 5:417–421.

Dickerson BC, Fenstermacher E, Salat DH, Wolk DA, Maguire RP, Desikan R, Pacheco J, Quinn BT, Van der Kouwe A, Greve DN, et al. 2008. Detection of cortical thickness correlates of cognitive performance: reliability across MRI scan sessions, scanners, and field strengths. Neuroimage. 39:10–18.

Dickerson BC, Goncharova I, Sullivan MP, Forchetti C, Wilson RS, Bennett DA, Beckett LA, deToledo-Morrell L. 2001. MRI-derived entorhinal and hippocampal atrophy in incipient and very mild Alzheimer's disease. Neurobiol Aging. 22:747–754.

Dickerson BC, Salat DH, Greve DN, Chua EF, Rand-Giovannetti E, Rentz DM, Bertram L, Mullin K, Tanzi RE, Blacker D, et al. 2005. Increased hippocampal activation in mild cognitive impairment compared to normal aging and AD. Neurology. 65:404–411.

Du AT, Schuff N, Kramer JH, Rosen HJ, Gorno-Tempini ML, Rankin K, Miller BL, Weiner MW. 2007. Different regional patterns of cortical thinning in Alzheimer's disease and frontotemporal dementia. Brain. 130:1159–1166.

Eickhoff SB, Heim S, Zilles K, Amunts K. 2006. Testing anatomically specified hypotheses in functional imaging using cytoarchitectonic maps. Neuroimage. 32:570–582.

Fagan AM, Mintun MA, Mach RH, Lee SY, Dence CS, Shah AR, LaRossa GN, Spinner ML, Klunk WE, Mathis CA, et al. 2006. Inverse relation between in vivo amyloid imaging load and cerebrospinal fluid Abeta42 in humans. Ann Neurol. 59:512–519.

Fischl B, Dale AM. 2000. Measuring the thickness of the human cerebral cortex from magnetic resonance images. Proc Natl Acad Sci USA. 97:11050–11055.

Fischl B, Liu A, Dale AM. 2001. Automated manifold surgery: constructing geometrically accurate and topologically correct models of the human cerebral cortex. IEEE Trans Med Imaging. 20: 70–80.

Fischl B, Sereno MI, Dale AM. 1999. Cortical surface-based analysis. II: Inflation, flattening, and a surface-based coordinate system. Neuroimage. 9:195–207.

Fischl B, Sereno MI, Tootell RB, Dale AM. 1999. High-resolution intersubject averaging and a coordinate system for the cortical surface. Hum Brain Mapp. 8:272–284.

Fotenos AF, Mintun MA, Snyder AZ, Morris JC, Buckner RL. 2008. Brain volume decline in aging: evidence for a relation between socioeconomic status, preclinical Alzheimer disease, and reserve. Arch Neurol. 65:113–120.

Fotenos AF, Snyder AZ, Girton LE, Morris JC, Buckner RL. 2005. Normative estimates of cross-sectional and longitudinal brain volume decline in aging and AD. Neurology. 64:1032–1039.

Fox NC, Scahill RI, Crum WR, Rossor MN. 1999. Correlation between rates of brain atrophy and cognitive decline in AD. Neurology. 52:1687–1689.

Frisoni GB, Testa C, Zorzan A, Sabattoli F, Beltramello A, Soininen H, Laakso MP. 2002. Detection of grey matter loss in mild Alzheimer's disease with voxel based morphometry. J Neurol Neurosurg Psychiatry. 73:657–664.

Gomez-Isla T, Price JL, McKeel DW, Jr, Morris JC, Growdon JH, Hyman BT. 1996. Profound loss of layer II entorhinal cortex neurons occurs in very mild Alzheimer's disease. J Neurosci. 16:4491–4500.

Good CD, Scahill RI, Fox NC, Ashburner J, Friston KJ, Chan D, Crum WR, Rossor MN, Frackowiak RS. 2002. Automatic differentiation of anatomical patterns in the human brain: validation with studies of degenerative dementias. Neuroimage. 17:29–46.

Gosche KM, Mortimer JA, Smith CD, Markesbery WR, Snowdon DA. 2002. Hippocampal volume as an index of Alzheimer neuropathology: findings from the Nun Study. Neurology. 58:1476–1482.

Han X, Jovicich J, Salat D, van der Kouwe A, Quinn B, Czanner S, Busa E, Pacheco J, Albert M, Killiany R, et al. 2006. Reliability of MRI-derived measurements of human cerebral cortical thickness: the effects of field strength, scanner upgrade and manufacturer. Neuroimage. 32:180–194.

Hyman BT, Van Hoesen GW, Damasio AR, Barnes CL. 1984. Alzheimer's disease: cell-specific pathology isolates the hippocampal formation. Science. 225:1168–1170.

Jack CR, Jr, Dickson DW, Parisi JE, Xu YC, Cha RH, O'Brien PC, Edland SD, Smith GE, Boeve BF, Tangalos EG, et al. 2002. Antemortem MRI findings correlate with hippocampal neuropathology in typical aging and dementia. Neurology. 58:750–757.

Jack CR, Jr, Petersen RC, O'Brien PC, Tangalos EG. 1992. MR-based hippocampal volumetry in the diagnosis of Alzheimer's disease. Neurology. 42:183–188.

Jack CR, Jr, Petersen RC, Xu YC, Waring SC, O'Brien PC, Tangalos EG, Smith GE, Ivnik RJ, Kokmen E. 1997. Medial temporal atrophy on MRI in normal aging and very mild Alzheimer's disease. Neurology. 49:786–794.

Juottonen K, Laakso MP, Insausti R, Lehtovirta M, Pitkanen A, Partanen K, Soininen H. 1998. Volumes of the entorhinal and perirhinal cortices in Alzheimer's disease. Neurobiol Aging. 19: 15–22.

Kabani N, Le Goualher G, MacDonald D, Evans AC. 2001. Measurement of cortical thickness using an automated 3-D algorithm: a validation study. Neuroimage. 13:375–380.

Karas GB, Burton EJ, Rombouts SA, van Schijndel RA, O'Brien JT, Scheltens P, McKeith IG, Williams D, Ballard C, Barkhof F. 2003. A comprehensive study of gray matter loss in patients with Alzheimer's disease using optimized voxel-based morphometry. Neuroimage. 18:895–907.

Karas GB, Scheltens P, Rombouts SA, Visser PJ, van Schijndel RA, Fox NC, Barkhof F. 2004. Global and local gray matter loss in mild cognitive impairment and Alzheimer's disease. Neuroimage. 23:708–716.

Killiany RJ, Gomez-Isla T, Moss M, Kikinis R, Sandor T, Jolesz F, Tanzi R, Jones K, Hyman BT, Albert MS. 2000. Use of structural magnetic resonance imaging to predict who will get Alzheimer's disease. Ann Neurol. 47:430–439.

Killiany RJ, Moss MB, Albert MS, Sandor T, Tieman J, Jolesz F. 1993. Temporal lobe regions on magnetic resonance imaging identify patients with early Alzheimer's disease. Arch Neurol. 50:949–954.
Klunk WE, Engler H, Nordberg A, Wang Y, Blomqvist G, Holt DP, Bergstrom M, Savitcheva I, Huang GF, Estrada S, et al. 2004. Imaging brain amyloid in Alzheimer's disease with Pittsburgh Compound-B. Ann Neurol. 55:306–319.
Kuperberg GR, Broome MR, McGuire PK, David AS, Eddy M, Ozawa F, Goff D, West WC, Williams SC, van der Kouwe AJ, et al. 2003. Regionally localized thinning of the cerebral cortex in schizophrenia. Arch Gen Psychiatry. 60:878–888.
Lerch JP, Pruessner JC, Zijdenbos A, Hampel H, Teipel SJ, Evans AC. 2005. Focal decline of cortical thickness in Alzheimer's disease identified by computational neuroanatomy. Cereb Cortex. 15:995–1001.
MacDonald D, Kabani N, Avis D, Evans AC. 2000. Automated 3-D extraction of inner and outer surfaces of cerebral cortex from MRI. Neuroimage. 12:340–356.
McKhann G, Drachman D, Folstein M, Katzman R, Price D, Stadlan EM. 1984. Clinical diagnosis of Alzheimer's disease: report of the NINCDS-ADRDA Work Group under the auspices of Department of Health and Human Services Task Force on Alzheimer's Disease. Neurology. 34:939–944.
Mesulam MM. 1998. From sensation to cognition. Brain. 121(Pt 6): 1013–1052.
Mintun MA, Larossa GN, Sheline YI, Dence CS, Lee SY, Mach RH, Klunk WE, Mathis CA, DeKosky ST, Morris JC. 2006. [11C]PIB in a nondemented population: potential antecedent marker of Alzheimer disease. Neurology. 67:446–452.
Morris JC. 1993. The Clinical Dementia Rating (CDR): current version and scoring rules. Neurology. 43:2412–2414.
Morris JC, Ernesto C, Schafer K, Coats M, Leon S, Sano M, Thal LJ, Woodbury P. 1997. Clinical dementia rating training and reliability in multicenter studies: the Alzheimer's Disease Cooperative Study experience. Neurology. 48:1508–1510.
Morris JC, McKeel DW, Jr, Fulling K, Torack RM, Berg L. 1988. Validation of clinical diagnostic criteria for Alzheimer's disease. Ann Neurol. 24:17–22.
Morris JC, Storandt M, Miller JP, McKeel DW, Price JL, Rubin EH, Berg L. 2001. Mild cognitive impairment represents early-stage Alzheimer disease. Arch Neurol. 58:397–405.
Morrison JH, Hof PR. 2002. Selective vulnerability of corticocortical and hippocampal circuits in aging and Alzheimer's disease. Prog Brain Res. 136:467–486.
Mueller SG, Weiner MW, Thal LJ, Petersen RC, Jack C, Jagust W, Trojanowski JQ, Toga AW, Beckett L. 2005. The Alzheimer's disease neuroimaging initiative. Neuroimaging Clin N Am. 15:869–877.
Murphy SN, Mendis ME, Grethe J, Gollub R, Kennedy D, Rosen BR. 2006. A web portal that enables collaborative use of advanced medical image processing and informatics tools through the Biomedical Informatics Research Network (BIRN). AMIA Annu Symp Proc. 579–583.
Price JL, Davis PB, Morris JC, White DL. 1991. The distribution of tangles, plaques and related immunohistochemical markers in healthy aging and Alzheimer's disease. Neurobiol Aging. 12:295–312.
Regeur L. 2000. Increasing loss of brain tissue with increasing dementia: a stereological study of post-mortem brains from elderly females. Eur J Neurol. 7:47–54.
Rosas HD, Liu AK, Hersch S, Glessner M, Ferrante RJ, Salat DH, van der Kouwe A, Jenkins BG, Dale AM, Fischl B. 2002. Regional and progressive thinning of the cortical ribbon in Huntington's disease. Neurology. 58:695–701.
Salat DH, Buckner RL, Snyder AZ, Greve DN, Desikan RS, Busa E, Morris JC, Dale AM, Fischl B. 2004. Thinning of the cerebral cortex in aging. Cereb Cortex. 14:721–730.
Scahill RI, Schott JM, Stevens JM, Rossor MN, Fox NC. 2002. Mapping the evolution of regional atrophy in Alzheimer's disease: unbiased analysis of fluid-registered serial MRI. Proc Natl Acad Sci USA. 99:4703–4707.
Scheff SW, DeKosky ST, Price DA. 1990. Quantitative assessment of cortical synaptic density in Alzheimer's disease. Neurobiol Aging. 11:29–37.
Schleicher A, Palomero-Gallagher N, Morosan P, Eickhoff SB, Kowalski T, de Vos K, Amunts K, Zilles K. 2005. Quantitative architectural analysis: a new approach to cortical mapping. Anat Embryol (Berl). 210:373–386.
Silbert LC, Quinn JF, Moore MM, Corbridge E, Ball MJ, Murdoch G, Sexton G, Kaye JA. 2003. Changes in premorbid brain volume predict Alzheimer's disease pathology. Neurology. 61:487–492.
Small GW, Kepe V, Ercoli LM, Siddarth P, Bookheimer SY, Miller KJ, Lavretsky H, Burggren AC, Cole GM, Vinters HV, et al. 2006. PET of brain amyloid and tau in mild cognitive impairment. N Engl J Med. 355:2652–2663.
Storandt M, Grant EA, Miller JP, Morris JC. 2002. Rates of progression in mild cognitive impairment and early Alzheimer's disease. Neurology. 59:1034–1041.
Storandt M, Grant EA, Miller JP, Morris JC. 2006. Progression in mild cognitive impairment (MCI) and PreMCI: a comparison of diagnostic criteria. Neurology. 67:467–473.
Terry RD, Masliah E, Salmon DP, Butters N, DeTeresa R, Hill R, Hansen LA, Katzman R. 1991. Physical basis of cognitive alterations in Alzheimer's disease: synapse loss is the major correlate of cognitive impairment. Ann Neurol. 30:572–580.
Thal LJ, Grundman M, Golden R. 1986. Alzheimer's disease: a correlational analysis of the Blessed Information-Memory-Concentration Test and the Mini-Mental State Exam. Neurology. 36:262–264.
Thompson PM, Hayashi KM, de Zubicaray G, Janke AL, Rose SE, Semple J, Herman D, Hong MS, Dittmer SS, Doddrell DM, et al. 2003. Dynamics of gray matter loss in Alzheimer's disease. J Neurosci. 23:994–1005.
Thompson PM, Mega MS, Woods RP, Zoumalan CI, Lindshield CJ, Blanton RE, Moussai J, Holmes CJ, Cummings JL, Toga AW. 2001. Cortical change in Alzheimer's disease detected with a disease-specific population-based brain atlas. Cereb Cortex. 11:1–16.
Tomlinson BE, Blessed G, Roth M. 1968. Observations on the brains of non-demented old people. J Neurol Sci. 7:331–356.
Van Hoesen GW, Hyman BT, Damasio AR. 1986. Cell-specific pathology in neural systems of the temporal lobe in Alzheimer's disease. Prog Brain Res. 70:321–335.
Whitwell JL, Shiung MM, Przybelski SA, Weigand SD, Knopman DS, Boeve BF, Petersen RC, Jack CR, Jr. 2008. MRI patterns of atrophy associated with progression to AD in amnestic mild cognitive impairment. Neurology. 70:512–520.
Wright CI, Dickerson BC, Feczko E, Negeira A, Williams D. 2007. A functional magnetic resonance imaging study of amygdala responses to human faces in aging and mild Alzheimer's disease. Biol Psychiatry. 62:1388–1395.
Wright CI, Feczko E, Dickerson B, Williams D. 2007. Neuroanatomical correlates of personality in the elderly. Neuroimage. 35:263–272.